LOCAL CONTRIBUTIONS TO THE 0.6 KEV DIFFUSE X-RAY BACKGROUND

David N. Burrows
Astronomy Department, The Pennsylvania State University

ABSTRACT

The intensity of the X-ray background between 0.5 and 1.0 keV has surprisingly little dependence on galactic latitude. Possible mechanisms for the production of these X-rays include extragalactic emission and emission from dM stars, both of which should be strongly dependent on galactic latitude, and diffuse emission from hot gas ($T \sim 3 \times 10^6$ K) surrounding the Sun. These mechanisms can be distinguished by the presence or absence of absorption by gas within a few hundred parsecs of the Sun. We use X-ray data from the HEAO-1 LED detectors and HI data from the recent Crawford Hill 21 cm survey to place limits on the 0.6 keV intensity originating within 300 pc of the Sun in the general direction of $(\ell,b) = (150°, -30°)$.

INTRODUCTION

The morphology of the X-ray diffuse background (XRB) varies greatly with energy. At energies above 2 keV, where the galactic plane is optically thin, the XRB is nearly isotropic, which implies that it is extragalactic in origin. At energies below 0.28 keV, where the mean free path is of order 100 pc, the XRB becomes highly anisotropic, and is generally thought to be primarily local in origin.

In the interval 0.5-1.0 keV, the source of the XRB is probably less well understood than in any other energy range. With the exception of several well-defined features produced by supernova remnants and hot cavities created by stellar winds or supernovae (e.g. the North Polar Spur and interior of Loop I, the Eridanus enhancement, the Cygnus Loop and Cygnus superbubble), the intensity of the XRB in this energy band is independent of galactic latitude (Nousek *et al.* 1982, Sanders *et al.* 1982). This is remarkable, because a mean free path for X-rays in this band is roughly a kiloparsec, so any non-local source mechanism (such as an extragalactic diffuse background, a hot halo, or emission from dM stars) should result in latitude-dependent intensity due to either emission or absorption in the galactic disk.

A model of the .6 keV XRB can be constructed that reproduces the latitude-independence of the data by balancing components from the three likely sources of emission: extragalactic flux, dM stars in the galactic plane, and local emission from hot gas (Burrows 1982, Sanders *et al.* 1982). This model requires a substantial contribution from the local region, suggesting the presence of gas with $T \sim 3 \times 10^6$ K within a few hundred parsecs of the Sun. An independent test for the presence of such gas in desirable.

https://doi.org/10.1017/S0252921100098213 Published online by Cambridge University Press

Local and non-local sources of diffuse X-rays can be distinguished observationally by the presence or absence of absorption by gas at a known distance. Such a test was performed by Bunner, Sanders, and Nousek (1979), using the SMC as an absorbing N_H feature. The results suggested that the X-rays originated on the near side of the SMC. (However, Seward and Mitchell (1981) found that this result could be influenced by unresolved X-ray sources in the SMC.) We use the same technique to look for evidence of the 0.6 keV absorption in nearby HI features.

DATA

The HEAO-1 A-2 LED experiment surveyed the sky in the energy range 0.18-3.0 keV. A map of a region centered on $(\ell,b) = (150°, -30°)$ was made for this analysis for an energy band with peak response at 0.62 keV. The angular resolution of the map is about 3° x 4°. The data used are from layer 1 of the LED detectors. Several stripes on the map parallel to the scan direction indicate that some of the data are contaminated by electrons or non-cosmic X-rays; these pixels were discarded. The response of the 0.6 keV band is shown in Figure 1. The absorption cross section for this energy band is about 6.7×10^{-22} cm^2 at unit optical depth, for the $E^{-1.4}$ power law spectrum of the 2-10 keV diffuse background.

We performed the analysis for two regions parallel to the galactic plane which include a wide range of N_H values. Region 1 is roughly bounded by $(142° < \ell < 165°)$, $(-27° < b < -15°)$. The Crawford Hill 21 cm survey (Stark et al. 1984) shows an N_H feature in region 1 with column densities of about 1.5×10^{21} cm^{-2}. Comparison of the 21 cm data with UV absorption data (Bohlin, Savage, and Drake 1978) and reddening data (FitzGerald 1968) suggests that the bulk of this gas is within 200-300 pc of the Sun. Region 2 is roughly bounded by $(140° < \ell < 175°)$, $(-46° < b < -38°)$. No UV absorption data and little reddening data are available for region 2, but the data available suggest that this gas may also be relatively close to the Sun.

In order to place limits on the fraction of the 0.6 keV intensity produced on the near side of this gas, a simple model was assumed for the 0.6 keV intensity. We assume that there are two emission components: an unabsorbed isotropic component, and an absorbed isotropic component. The model is given by

$$I(\ell,b) = I_L + I_D \exp(-\sigma N_H(\ell,b)),$$

where I_L is the local component, I_D is the distant component, σ is the cross section, and N_H is the measured HI column density.

RESULTS

The results of the model fitting in region 1 are shown in Figure 2. The solid line is the best-fit model ($I_L = 1.3$, $I_D = 6.5$, $\chi^2_\nu = 5.3$), while the dashed and dotted lines represent the cases of purely local ($I_L = 4.3$, $I_D =$

https://doi.org/10.1017/S0252921100098213 Published online by Cambridge University Press

0.0, χ^2_ν = 8.7) and purely distant (I_L = 0.0, I_D = 9.2, χ^2_ν = 5.52) emission, respectively. Clearly, none of the fits are very good, but the fits with substantial fractions of the X-rays coming from beyond the gas are significantly better than that in which all of the X-rays originate locally. The poor fits may be due to small-scale structure in the emission region or to residual contamination in the data. Unfortunately, the quality of the fits does not permit the model parameters to be constrained in a statistically valid way. However, it is probably fair to conclude that the evidence favors a distant, rather than local, origin of these X-rays.

The opposite conclusion is reached from the data in region 2. The results are shown in Figure 3. Again, the solid line is the best-fit model (I_L = 3.6, I_D = 1.5, χ^2_ν = 1.9), the dashed line is local (I_L = 4.4, I_D = 0.0, χ^2_ν = 2.1), and the dotted line is distant (I_L = 0.0, I_D = 7.6, χ^2_ν = 5.4). These fits indicate that most or all of the X-rays come from the near side of the gas. This result suggests that the extragalactic power law observed at high energies does not continue below 1 keV. It is not completely clear whether it implies a truly local source of 0.6 keV X-rays, however, because the location of the absorbing gas in region 2 is not well established. If this gas is as much as a kiloparsec away, the results from region 2 may be consistent with those from region 1, where the gas is known to be close, if the X-rays are coming from fairly distant regions rather than from the local cavity that produces the 1/4 keV XRB in these regions.

ACKNOWLEDGEMENTS

George Weaver was responsible for producing the maps. John Nousek provided advice on processing the data. Carl Heiles kindly provided the Crawford Hill 21 cm data before publication. This work was supported by NASA grant NAS5-26809.

REFERENCES

Burrows, D.N. 1982, Ph.D. Thesis, University of Wisconsin-Madison.
Bohlin, R.C., Savage, B.D., and Drake, J.F. 1978, Ap.J., 224, 132.
FitzGerald, M.P. 1968, Astron. J., 73, 983.
Nousek, J.N., Fried, P.M. Sanders, W.T., and Kraushaar, W.L. 1982, Ap.J., 258, 83.
Sanders, W.T., Burrows, D.N., Kraushaar, W.L., and McCammon, D. 1982, in IAU Symposium #101, Supernova Remnants and their X-ray Emission, ed. P. Gorenstein and J. Danziger (Dortrecht:Reidel).
Seward, F.D., and Mitchell, M. 1981, Ap. J., 243, 736.
Stark, A.A., Heiles, C., Bally, J., and Linke, R. 1984, in preparation.

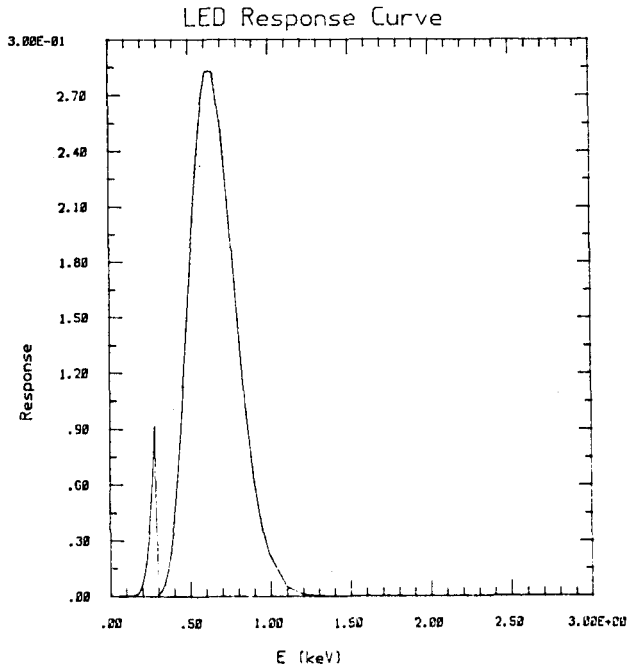

Fig. 1

Fig. 1 - Response curve for the 0.6 keV band used for this analysis.

Fig. 2 - Data and models for region 1. Details given in text.

Fig. 3 - Data and models for region 2. Details given in text.

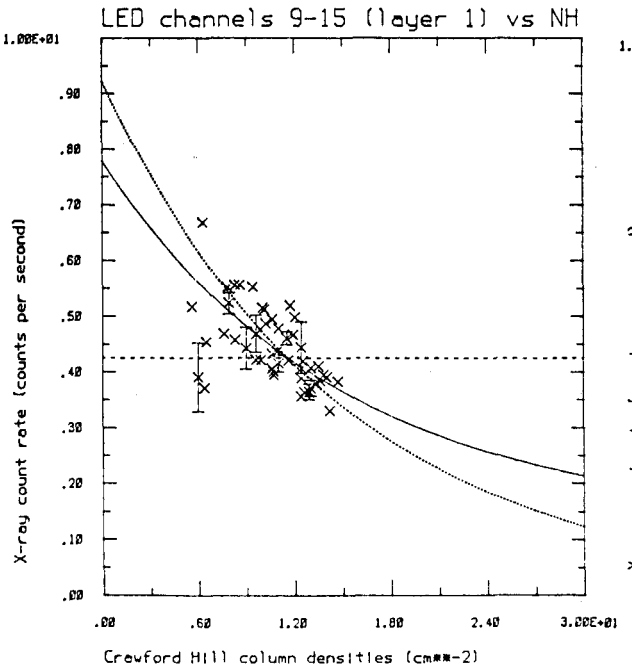

Fig. 2

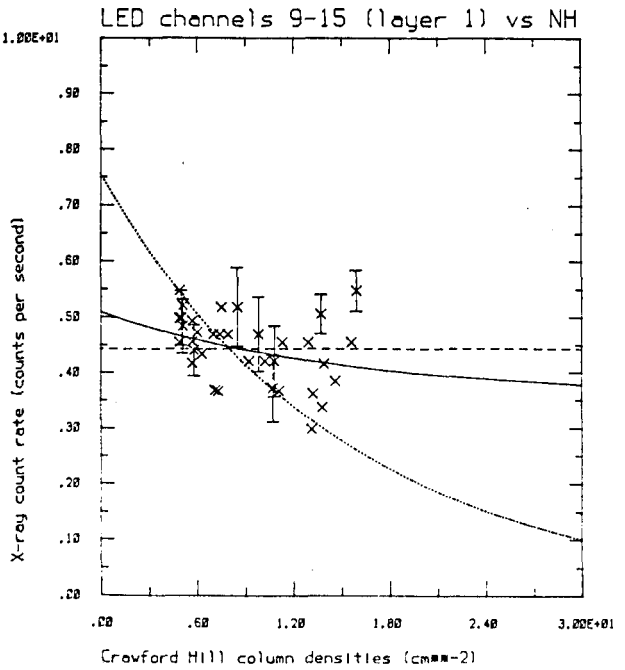

Fig. 3

https://doi.org/10.1017/S0252921100098213 Published online by Cambridge University Press